Journal of
Materials Chemistry B

Accepted Manuscript

This article can be cited before page numbers have been issued, to do this please use: A. Lancelot, R. González, R. Clavería-Gimeno, P. Romero, O. Abian, P. Martin-Duque, J. L. Serrano and T. Sierra, *J. Mater. Chem. B*, 2018, DOI: 10.1039/C8TB00639C.

ROYAL SOCIETY OF CHEMISTRY

rsc.li/materials-b

View Article Online
DOI: 10.1039/C8TB00639C

Journal Name

ARTICLE

Cationic poly(ester amide) dendrimers: alluring materials for biomedical applications

Received 00th January 20xx,
Accepted 00th January 20xx

DOI: 10.1039/x0xx00000x

www.rsc.org/

Alexandre Lancelot,[a‡] Rebeca González-Pastor,[b,c‡] Rafael Clavería-Gimeno,[c,d] Pilar Romero,[e] Olga Abian,[b,c,d,f] Pilar Martín-Duque,[b,c*] José L. Serrano,[a*] Teresa Sierra.[e*]

Novel cationic poly(ester amide) dendrimers have been synthesized by copper(I) azide-alkyne cycloaddition (CuAAC) of a tripropargyl amine core and azide-terminated dendrons, in turn prepared by iterative amide coupling of the new monomer 2,2'-*bis*(glycyloxymethyl)propionic acid (*bis*-GMPA). The alternation of ester and amide groups provided a dendritic scaffold that was totally biocompatible and degradable in aqueous media at physiological and acidic pH. The tripodal dendrimers naturally formed rounded aggregates with a drug that had low water solubility, camptothecin, thus improving its cell viability and anti-Hepatitis C virus (anti-HCV) activity. The presence of numerous peripheral cationic groups enabled these dendrimers to form dendriplexes with both pDNA and siRNA and these showed effective *in vitro* siRNA transfection in tumoral and non-tumoral cell lines.

Introduction

Synthetic vectors applied to drug delivery and gene therapy offer new opportunities to cure diseases in very specific and efficient way. The conjugation of drugs with a vector may modify the pharmacokinetic profiles and improve various key parameters, such as their bioavailability, biodistribution and activity, thus limiting drug doses and undesired side effects.[1-3] The delivery of exogenous genetic material into cells upon conjugation with a vector may favour the production of a missing protein, silence the expression of a deleterious gene or specific cell suicide to cure the diseases in a highly precise way.[4,5] In order to perform these activities, the biocompatibility and degradability in physiological media of the synthetic vector is a crucial issue that must be considered in their design.[6]

Among synthetic vectors, dendrimers show interesting features that have prompted their development for biomedical applications. Indeed, these monodisperse macromolecules have a globular shape that favours the presence of numerous and available functional groups at their surface. These groups can be easily modified with biological moieties, targeting molecules or dyes, amongst other units, in order to turn a dendrimer into a multifunctional platform that is able to transport drugs and/or genes, which is useful from investigation to clinical applications.[7-11]

Commercially available poly(amidoamine) (PAMAM) and poly(propylene imine) (PPI) dendrimers are the most commonly used systems for these two applications. The numerous nitrogen functional groups that make up the dendrimers favour their entry into the cell cytoplasm, where they can release their pharmaceutical cargo. These two systems have demonstrated impressive abilities to improve drug activity and to enhance gene transfection.[12,13,14] Unfortunately, the weak biocompatibility and degradability of these functional groups induce a cytotoxic effect that must be tempered, usually by the addition of polyethylene glycol on the dendrimer surface.[15,16,17] Dendrimers based on oxygen functions, such as 2,2'-*bis*(hydroxymethyl)propionic acid (*bis*-MPA) polyester dendrimers[18] or polyglycerol polyether dendrimers,[19] have also been investigated for the purposes outlined above as they present excellent biocompatibility and can be rapidly degraded in physiological media. However, these materials generally show less marked biological improvement than PAMAM and PPI derivatives, especially in gene transfection.[20]

a Instituto de Nanociencia de Aragón (INA), Universidad de Zaragoza, Spain
b Aragon Institute for Health Research (IIS Aragon), Zaragoza, Spain.
c Instituto Aragonés de Ciencias de la Salud (IACS), Zaragoza, Spain.
d Institute of Biocomputation and Physics of Complex Systems (BIFI), Joint Unit IQFR-CSIC-BIFI, Universidad de Zaragoza, Spain
Instituto de Ciencia de Materiales de Aragón (ICMA), Facultad de Ciencias, Universidad de Zaragoza-CSIC, Spain
f Centro de Investigación Biomédica en Red en el Área Temática de Enfermedades Hepáticas y Digestivas (CIBERehd), Barcelona, Spain.
g Fundación ARAID, Government of Aragon, Zaragoza, Spain,
‡ These authors contributed equally to the work. *Email - tsierra@unizar.es

Electronic Supplementary Information (ESI) available: [Detailed protocols carried out for the anti-HCV studies and for the pDNA transfection. Synthesis and characterization of the bis-GMPA monomer. Dendrons and dendrimers. Biocompatibility of the dendrons and dendrimers and degradability of the dendrons. Characterization of complexes formed between *bis*-GMPA dendrimers and pEGFP. SI7. siRNA transfection efficacy of commercial reagents.]. See DOI: 10.1039/x0xx00000x

View Article Online
DOI: 10.1039/C8TB00639C

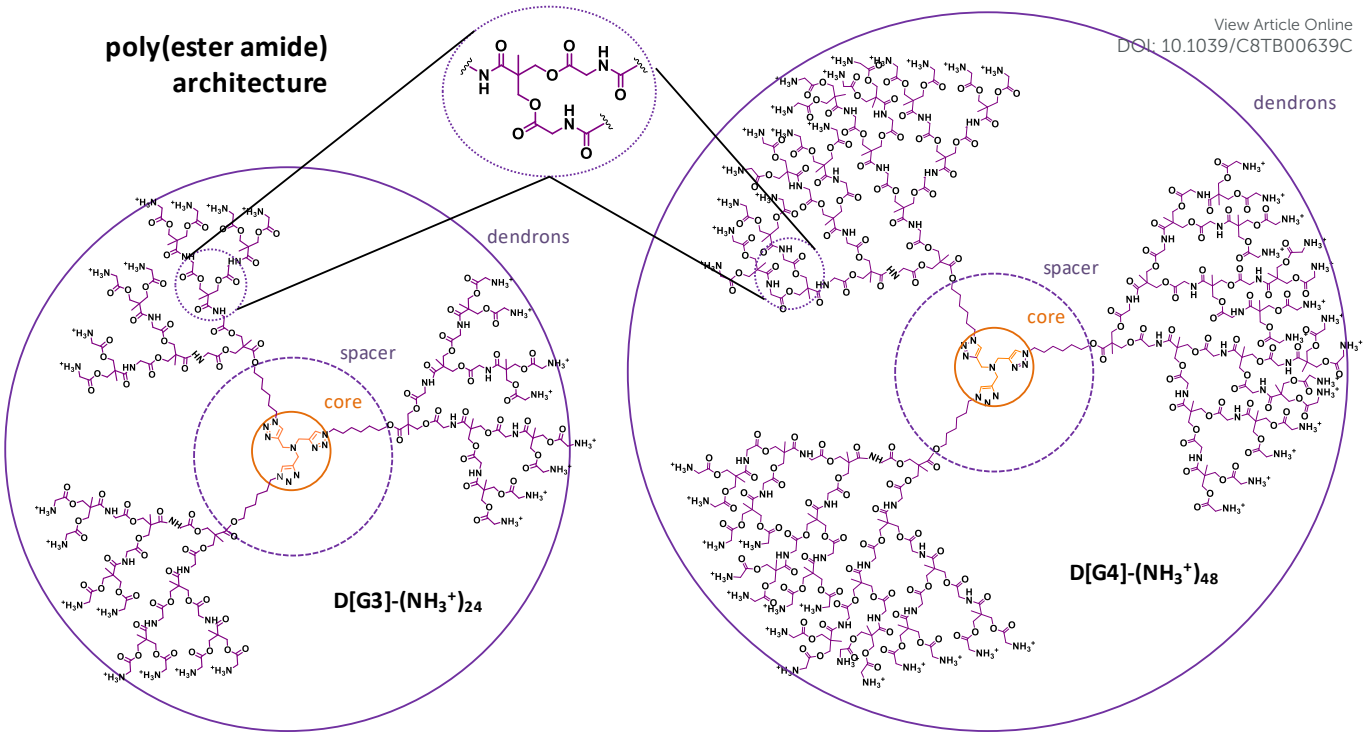

Figure 1. 2,2'-*bis*(glyciloxy)propionic acid (*bis*-GMPA) dendrimers of 3rd and 4th generation.

In order to combine the advantages of nitrogen and oxygen functions in the chemical structure of dendrimers, hybrid structures containing ether and imine groups, such as poly(propyl ether imine) (PETIM) dendrimers, have been studied in both gene[21] and drug delivery[22] applications along with structures with ether and amide groups such as gallic acid-triethylene glycol (GATG) dendrimers.[23] Although linear poly(ester amide) polymers have shown interesting results for biomedical applications,[24] poly(ester amide) dendrimers are still sporadic. The combination of the hydrolytic degradability of ester linkages and the stability and H-bond-forming ability of amido groups makes these polymers attractive candidates to form synthetic vectors for drug and gene delivery. Furthermore, the inclusion of amino acids as a source of amino groups imparts poly(ester amide)s with additional advantages in terms of their biological properties. To our knowledge, only a poly(ester amide) dendrimer can be found in the literature, and this is based on glycine and *bis*-MPA monomer. This material was synthesized by iterative esterification couplings and it has terminal hydroxyl groups, which help to improve the water solubility of glymepiride, an antidiabetic drug low-water.[25]

We present here a novel 2,2'-*bis*(glycyloxymethyl)propionic acid (*bis*-GMPA) monomer that allows the synthesis of poly(ester amide) dendrons with terminal amino groups. We have previously reported the potential of glycyloxy amino-terminated dendrons and dendrimers with a *bis*-MPA polyester skeleton that formed biocompatible nanocarriers for drug delivery[26,27] and/or gene transfection.[20,28] The amino groups corresponded in all cases to glycine moieties and these provided a dendritic scaffold that releases non-toxic glycine and *bis*-MPA molecules upon degradation. As a continuation of our investigation of such amino-terminated carriers, we have implemented a synthetic procedure that involves iterative amidation coupling reactions that lead to poly(ester amide) dendrons containing glycine and *bis*-MPA. The 3rd and 4th generation dendrons with 8 and 16 terminal ammonium groups, respectively, were thus prepared and grafted onto a tripropargyl amine core in order to obtain flexible tripodal poly(ester amide) dendrimers (Figure 1). The biocompatibility and degradability in aqueous media of such structures were confirmed as along with their potential to deliver an anti-hepatitis C virus (anti-HCV) drug with low-water soluble as well as plasmid deoxyribonucleic acid (pDNA) and small interfering ribonucleic acid (siRNA).

Results and discussion

Synthesis and chemical characterization

View Article Online
DOI: 10.1039/C8TB00639C

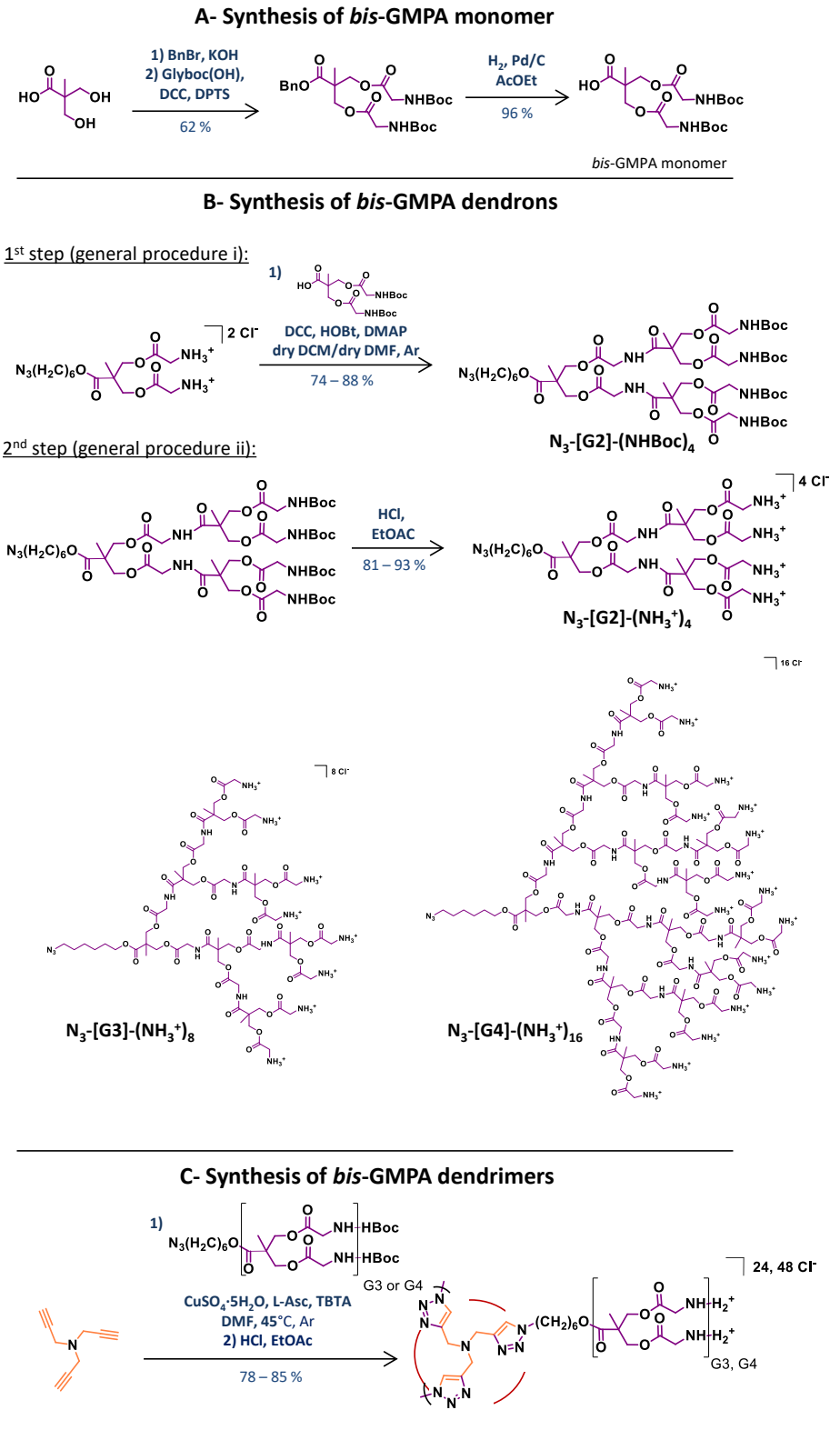

Scheme 1. Synthesis of: (A) *bis*-GMPA monomer (Bn = benzyl), (B) Dendrons. The two-step procedure followed to grow the dendron generation is represented for the synthesis of the 2nd generation dendron, N_3-[G2]-$(NH_3^+)_4$. The chemical structures of 3th and 4th generation dendrons used to synthesize the final dendrimers are represented. (C) Dendrimers.

View Article Online
DOI: 10.1039/C8TB00663C

The 2nd, 3rd and 4th generation *bis*-GMPA dendrons were synthesized starting from 6-azidohexyl *bis*(hydroxymethyl) propionate, previously described by us.[31] This compound was functionalized with *t*-Boc-glycine moieties, as described for the *bis*-GMPA monomer (Scheme 1A), and subsequent amino group deprotection (see Scheme SI.3.2). The dendron generation was grown by employing repetitive amidation coupling reactions using dicyclohexylcarbodiimide (DCC), 1-hydroxybenzotriazole hydrate (HOBt) and 4-(dimethylamino) pyridine (DMAP) with a mixture of dry dichloromethane and dry dimethylformamide as solvent (Scheme 1B). Subsequent deprotection of the terminal amino groups was carried out under acidic conditions (3M HCl in ethyl acetate). Under these conditions the terminal amines form the ammonium salt and this precipitates from the reaction mixture. The precipitation allows an easy purification process and protects the internal amide and ester groups of the dendron from acidic hydrolysis. This two-step growth procedure, i.e. amido coupling and deprotection, gaved the products in yields between 62 and 78 %.

Finally, the tripodal dendrimers of 3rd and 4th generation, **D[G3]-(NH_3^+)$_{24}$** and **D[G4]-(NH_3^+)$_{48}$**, respectively, were obtained by coupling three dendrons on the tripropargyl amine core by means of copper(I) azide-alkyne cycloaddition (CuAAC) (Scheme 1C). Given the high conversion yields and the low number of by-products generated, CuAAC "click-chemistry" has been used for the synthesis of tripodal dendrimers with *tris*(alkyne)-derived cores,[32] but the tripropargyl amino core has rarely been used.[33] In order to favour the complete functionalization of the core and impart flexibility to the final dendritic structures, an hexamethylenic chain was included as a spacer between the core and the *bis*-GMPA dendron. This reaction was carried out with the *t*-Boc protected dendrons in order to avoid undesired copper complexation by the dendrons, which may lower the reaction yields, and to simplify the purification of the dendrimers. Copper(I) was prepared *in situ* by reduction of copper(II) sulfate by (*L*)-sodium ascorbate and tris[(1-benzyl-1*H*-1,2,3-triazol-4-yl)methyl]amine (TBTA), which was added to the reaction mixture to increase its stability. Once again, the *t*-Boc protective groups were removed under acidic conditions in ethyl acetate to obtain defect-free *bis*-GMPA dendrimers of 3rd and 4th generation, which contained 24 and 48 terminal ammonium groups and 18 and 46 internal amide groups, respectively, and these were obtained in yields of 85 and 78 %.

At the end of the synthesis, the amount of copper that might have remained in the dendrimers, and which could provoke cytotoxic bioaccumulation, was measured by inductively coupled plasma atomic emission spectroscopy (ICP-AES). The amounts of copper that remained in the two final compounds were extremely low, 16 and 54 μg/g for **D[G3]-(NH_3^+)$_{24}$** and **D[G4]-(NH_3^+)$_{48}$**, respectively, i.e., far below the value of the recommended dietary allowance of copper.[34]

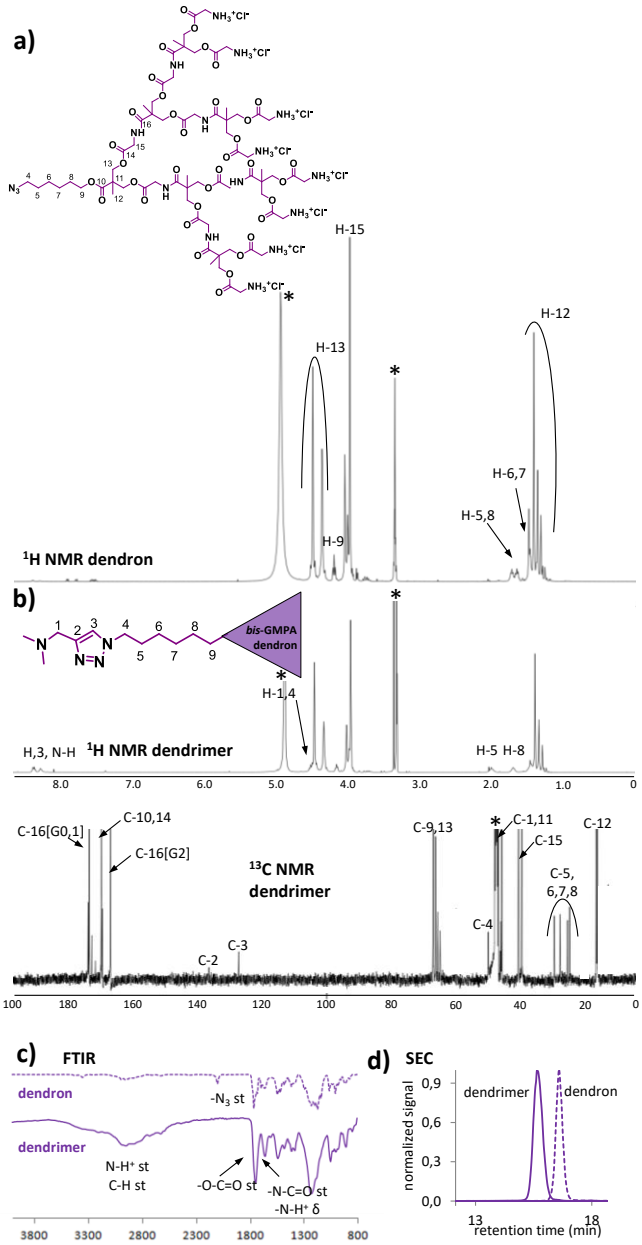

Figure 2. Chemical structures and characterization of the 3rd generation *bis*-GMPA dendron, **N_3-[G3]-(NH_3^+)$_8$**, and dendrimer **D[G3]-(NH_3^+)$_{24}$**. a) ^{1}H NMR of the *bis*-GMPA dendron in CD_3OD, b) ^{1}H and ^{13}C NMR of dendrimer **D[G3]-(NH_3^+)$_{24}$** in CD_3OD, c) FTIR spectra of the dendron and the dendrimer and d) SEC chromatogram of the dendron and dendrimer with terminal *t*-Boc groups. * asterisks indicate solvent signals.

View Article Online
DOI: 10.1039/C8TB00639C

The ^{1}H-NMR spectrum of the 3rd generation *bis*-GMPA dendron, **N$_3$-[G3]-(NH$_3^+$)$_8$**, is depicted in Figure 2a as an example to illustrate the correct synthesis of the dendron. The signals corresponding to the glycine methylenic groups, *H-15*, are observed as singlets between 3.6 and 4.0 ppm and the oxymethylene protons, *H-13*, appear as ABq signals between 3.6 and 4.6 ppm. The signals corresponding to the 6-azidohexyloxy chain are also observed at 1.43-1.69 ppm (*H-5 to H-8*) and at 4.16 ppm (*H-9*), except for the triplet corresponding to the methylenic protons, *H-4*, which appears overlapped with the signal of the solvent. Nevertheless, the correlation of this triplet with the signal corresponding to its vicinal methylenic protons *H-5* could be observed in ^{1}H-^{1}H COSY spectrum (see Figure SI.3.1). Additionally, the chemical structure, monodispersity and purity of each dendron were confirmed by Fourier transform infrared (FTIR) spectroscopy, mass spectrometry (MALDI-TOF), size exclusion chromatography (SEC) and elemental analysis (EA). Mass spectrometry and SEC results for each dendron whose terminal amino groups were protected by *t*-Boc are gathered in the supporting information (see Figure SI.3.2).

The ^{1}H NMR, ^{13}C NMR and FTIR spectra, as well as the SEC chromatograms, of the 3rd generation tripodal dendrimer, **D[G3]-(NH$_3^+$)$_{24}$**, are also depicted in Figure 2 as a representative example. The correct synthesis of the dendrimer was confirmed by the appearance of the signals corresponding to the formation of the triazole ring between the tripropargyl core and the dendrons, i.e., a peak at 8.42 ppm in the ^{1}H NMR spectrum corresponding to the proton *H-3* and two peaks at 128.7 and 137.9 ppm in the ^{13}C NMR spectrum corresponding to carbons *C-3* and *C-2,* respectively. Additionally, the signals corresponding to the methylenic protons adjacent to the triazole ring, *H-4* and *H-5*, were shifted downfield, moving from 3.23 to 4.52 ppm and from 1.62 to 1.99 ppm, respectively. The protons of the tripropargyl amino core appeared at 4.52 ppm in a merged signal. The correct assignment of the proton and carbon signals was confirmed by ^{1}H-^{1}H COSY and ^{1}H-^{13}C HSQC experiments (Figures SI.4.1. and SI.4.2.). In the FTIR spectra, the band corresponding to the azide group dissappeared after the CuAAC reaction. Characteristic bands of ester, amide and protonated amino groups were observed, respectively, at 1749, 1655 and as a broad signal between 3600 and 2600 cm^{-1} (Figure 2C). The monodispersity was confirmed by SEC, which provided chromatograms in which the retention time decreased after the CuAAC reaction and a residual peak corresponding to uncoupled free dendrons could not be observed (Figure 2D and Figure SI.4.3.).

Biocompatibility and Degradability

As a first criterion to assess the potential of these cationic poly(ester amide) dendrons and dendrimers for biomedical applications, their biocompatibility and degradability were assessed.

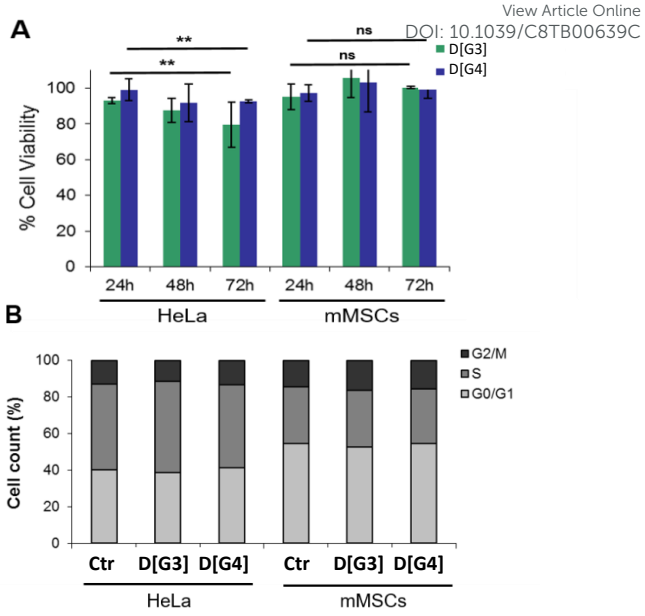

Figure 3. Cytotoxicity of the dendrimers, **D[G3]-(NH$_3^+$)$_{24}$** and **D[G4]-(NH$_3^+$)$_{48}$**, on HeLa and mMSCs. A. Cell viability after incubation with 1 mg/mL of *bis*-GMPA dendrimers was analysed by the Alamar Blue® assay and the fluorescence was normalized to cells receiving medium alone (** $p < 0.01$, ns not significant). B. Effect of 1 mg/mL of exposure for 24 h on the phases of the cell cycle.

The biocompatibility of dendrons and dendrimers was studied in tumoral cells (HeLa) and mesenchymal stem cells of mouse origin (mMSCs) (Figure 3 and SI.5.1.1-2). Cell viability remained constant for normal mMSCs (> 95%), whereas a decrease was observed on tumoral HeLa cells between 24 h and 72 h. In any case, all of the dendrons and dendrimers showed cell viability values above 70% for the two cell lines for concentrations up to 1 mg/mL, even after 72 hours (Figure 3A), thus confirming their biocompatibility. Moreover, significant changes were not found in cell cycle distribution (Figure 3B).

The degradability of the *bis*-GMPA dendrons, **N$_3$-[G2]-(NH$_3^+$)$_4$**, **N$_3$-[G3]-(NH$_3^+$)$_8$** and **N$_3$-[G4]-(NH$_3^+$)$_8$** was studied by ^{1}H NMR experiments in aqueous buffer at pH = 7.4, i.e., physiological pH, and at pH = 5.0, which corresponds to the pH observed in the late endosomes. The most revealing zones of the proton spectra corresponding to the degradation study of **N$_3$-[G2]-(NH$_3^+$)$_4$** at different times are shown in Figure 4. The ^{1}H NMR spectra for the degradation study of **N$_3$-[G3]-(NH$_3^+$)$_8$** and **N$_3$-[G4]-(NH$_3^+$)$_{16}$** are gathered in Figures SI5.2.

At pH = 7.4, new signals near 3.6 ppm appeared over time. These signals correspond to hydroxymethylenic protons, i.e. –C*H*$_2$OH, as described previously,[31] and arise from the slow hydrolysis of the external ester functions, which release glycine units into the medium. This interpretation was corroborated by the modifications observed near 3.84 ppm, which are consistent with the appearance of methylenic protons of free glycine. Additionally, the proton signals corresponding to the C*H*$_2$-OC(O) and N*H*C(O) groups at 4.20-4.40 and 8.30 ppm, respectively, are modified during the hydrolysis process. All of the changes outlined above occur slowly since the signals become clearly visible between 2 and 7 days.

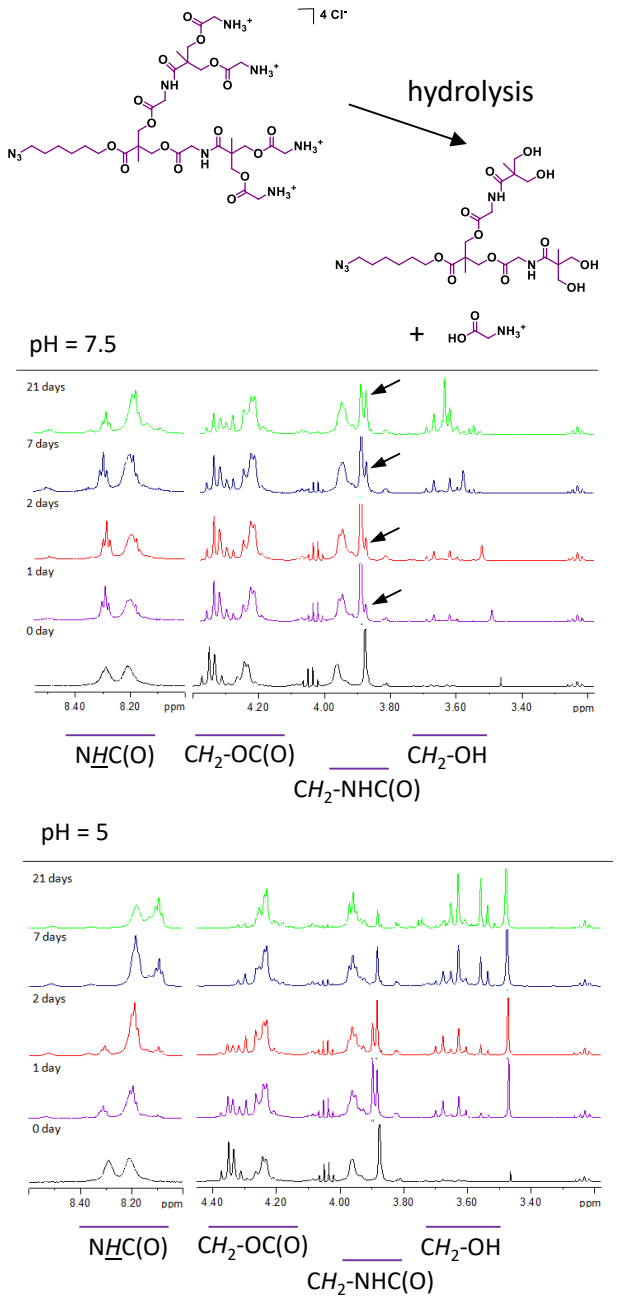

Figure 4. Degradation of the *bis*-GMPA dendron **N_3-[G2]-(NH_3^+)$_4$** in aqueous buffers at pH = 7.4 and 5.

At acidic pH (i.e. 5.0), the degradation of the dendrons by hydrolysis was clearly accelerated and, after the first day, signals at around 3.6 ppm, corresponding to C*H*$_2$OH protons, were visible. All of the peripheral glycine moieties were then totally released after one week. After this first step, the dendron degradation continued, as evidenced by the appearance of peaks with lower intensity close to 3.78 ppm and by the modifications of the remaining signals close to 4.25 ppm (*CH*$_2$-OC(O) area) and 8.15 ppm (N*H*C(O) area).

Drug delivery

The possibility of using these poly(ester amide) dendrimers as carriers to improve the activity of small drugs was initially tested in anti-hepatitis C virus (anti-HCV) experiments for the dendrimer **D[G3]-(NH_3^+)$_{24}$** using camptothecin (CPT). Indeed, CPT was previously identified as a potential inhibitor of the virus replication during in vitro assays.[35] Although CPT is highly toxic, it has previously been reported that its encapsulation within organic nanostructures can improve its anti-HCV activity while preserving cell viability.[27,36,37]

The procedure based on the solvent diffusion technique for drug loading was employed to prepare dendrimer-drug complexes with a ratio of 58 µmol CPT/mol dendrimer. Although this drug content is not high, we found that in the presence of dendrimer the CC50 referred to CPT was higher than 1 µM, compared to 0.5 µM for free CPT. At the same time, viral inhibition at a 0.01 µM concentration of CPT increased from 50% using free CPT to 80% for **D[G3](NH_3^+)$_{24}$/CPT** (Figure 5). These data showed that CPT was more active and less cytotoxic when offered to infected cells associated with the dendrimer.

The dendrimer-drug system was studied by TEM (Figure 5) and this showed rounded objects with a mean size of 21 ± 5 nm, which is twice the size of the nanoobject formed by the empty dendrimer (10 ± 3 nm). Furthermore, Isothermal Titration Calorimetry (ITC) measurements showed that CPT-dendrimer association is energetically favoured with an association constant of $K_a = 4.1 \pm 0.6 \cdot 10^6$ M^{-1}. This value corresponds to a moderate to high Gibbs energy of interaction (ΔG= -8.9 ± 0.8 kcal·mol^{-1}) dominated by the entropic contribution ($-T\Delta S$= –9.9 ± 0.9 kcal·mol^{-1}), with an unfavourable interaction enthalpy (ΔH= 0.9 ± 0.1 kcal·mol^{-1}). This could mean that drug and dendrimer binding is led by non-specific interactions (mainly hydrophobic forces), which is consistent with the drug being encapsulated within the dendritic nano-objects observed by TEM, and this allows its cell viability and antiviral activity to be enhanced.

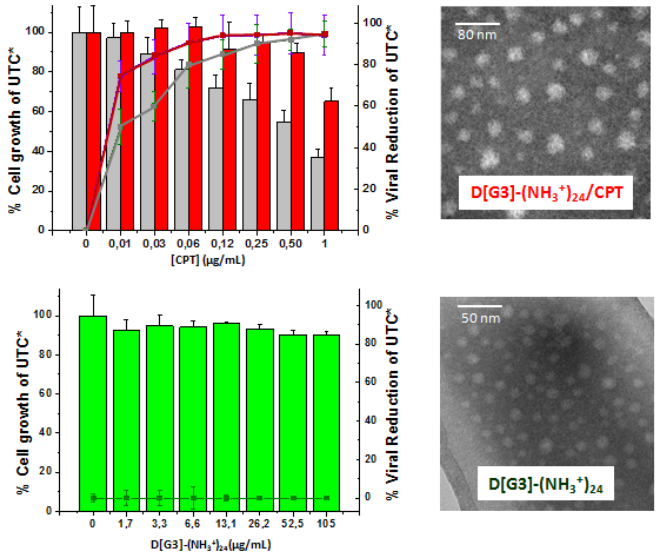

Figure 5. Evaluation of viral load reduction (lines) of HCV replicon system in human hepatoma cells (Huh5-2) with cell growth (bars) while increasing compound concentration and TEM images of **D[G3](NH_3^+)$_{24}$/CPT** (red) and **D[G3](NH_3^+)$_{24}$** (green); **free CPT** (grey) is represented as a control in **D[G3](NH_3^+)$_{24}$/CPT** graph. *UTC: untreated controls.

pDNA and siRNA dendriplexes formation and transfection

The potential of the novel cationic *bis*-GMPA poly(ester amide) dendrimers to be used as non-viral gene vectors was investigated with pDNA (pEGFP) and siRNA (siGFP and siLuc). GFP and firefly luciferase are widely used as reporters to study gene expression. The GFP system is based on the production of a green fluorescence protein that can be detected after its transfer, and the luciferase system is based on bioluminescence, where the enzyme luciferase catalyses a two-step reaction in which oxidation of D-luciferin yields light. Although it is more common to use the transfer of pDNA encoding a protein that is missing or defective into a patient's cells, in the last few years there has been considerable interest in the use of short double-stranded RNAs in gene therapy, as there is evidence for the inhibition of proliferation of tumour cells by sequence-specific silencing of factors that support tumour growth or facilitate the generation of chemotherapy-resistant cells.[38-41]

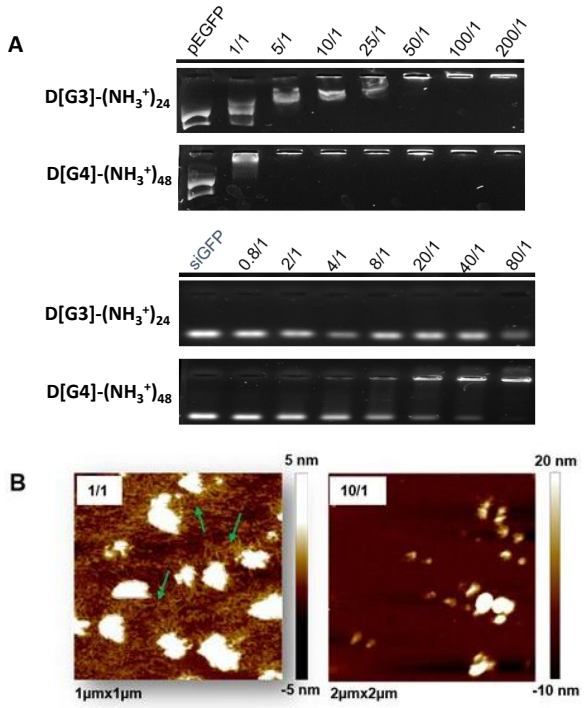

Figure 6. A. Electrophoretic mobility of free and complexed pDNA and siRNA in SFM. Gel retardation of pDNA (up) and siRNA (down) in the presence of increasing concentrations of **D[G3]-$(NH_3^+)_{24}$** and **D[G4]-$(NH_3^+)_{48}$** (D[G3]-$(NH_3^+)_{24}$, 6256 g/mol, 24 N^+/molecule; D[G4]-$(NH_3^+)_{48}$, 12671 g/mol, 48 N^+/molecule; pEGFP, $3.12 \cdot 10^6$ g/mol, 9400 P^-/molecule; siGFP 14520 g/mol, 44 P^-/molecule). B. AFM images of dendriplexes formed between **D[G4]-$(NH_3^+)_{48}$** and pDNA at 1/1 and 10/1 w/w ratios. Free pDNA chains are highlighted with green arrows.

Gel electrophoresis results (Figure 6A) showed differences in the complexation capacity of the two dendrimers, with **D[G4]-$(NH_3^+)_{48}$** being the most efficient to spontaneously form dendriplexes with either pDNA or siRNA. As for pDNA complexation, a w/w ratio of 5/1 for pDNA (N/P ratio 6.3) was observed whereas the ratio was 50/1 for **D[G3]-$(NH_3^+)_{24}$**. As for siRNA complexation, a w/w ratio of 80 for pDNA (N/P ratio 100/1) was deduced for the largest dendrimer, **D[G4]-$(NH_3^+)_{48}$**, and siRNA complexation was not observed for the smallest dendrimer. Accordingly, the number of peripheral amines in the dendrimer seems to be crucial to enhance good complexation abilities at low ratios.[42] For these reasons, **D[G4]-$(NH_3^+)_{48}$** was chosen to explore further the transfection efficiency of its corresponding dendriplexes with pEFGP and siGFP.

The correct formation of the dendriplexes with **D[G4]-$(NH_3^+)_{48}$** and pDNA was confirmed by AFM (Figure 6B). At low ratios (w/w 1/1), free pDNA appears as fibres with a low height (around 0.7 nm), whereas at higher ratios (w/w 10/1) these fibres are no longer observed and only rounded dendriplexes are visible. This is consistent with the results obtained during gel electrophoresis experiments (Figure 6A).

Morphological studies of the dendriplexes were carried out by cryoTEM at different w/w ratios (Figure 7 and Table 1), and their hydrodynamic size and superficial charge were measured by DLS and ζ potential measurements (Table 1). **D[G4]-$(NH_3^+)_{48}$** forms spherical objects when mixed with pDNA. the addition of further quantities of dendrimer (ratio 100/1) allows the formation of smaller and less polydisperse dendriplexes. When mixed with siRNA, spherical dendriplexes were observed at the lowest ratio (50/1). The addition of a larger quantity of dendrimer (ratio 100/1) triggered the formation of bigger and more elongated objects. All of the dendriplexes showed a positive superficial charge that increased on the addition of dendrimer.

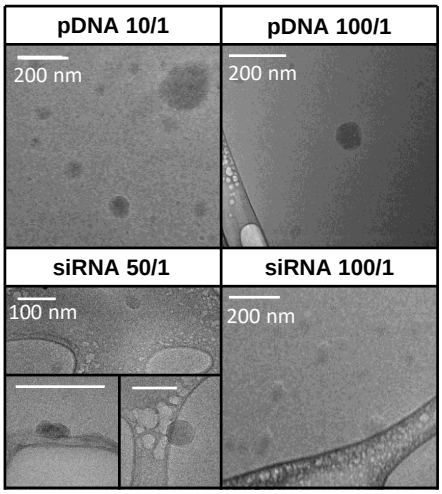

Figure 7. CryoTEM images of the dendriplexes formed by **D[G4]-$(NH_3^+)_{48}$** when mixed with pDNA or siRNA.

Table 1. Diameter (D_H) and ζ potential values of the dendriplexes.

Dendriplexes	D_H (nm)		ζ potential (mV)
	DLS	cryoTEM	
D[G4]-$(NH_3^+)_{48}$/pDNA 10/1	57 ± 4 244 ± 21	30 - 70 120 - 200	+ 12
D[G4]-$(NH_3^+)_{48}$/pDNA 100/1	85 ± 22	30 - 120	+ 23
D[G4]-$(NH_3^+)_{48}$/siRNA 50/1	63 ± 9	35 - 60	+ 19
D[G4]-$(NH_3^+)_{48}$/siRNA 100/1	179 ± 29	50 -120	+21

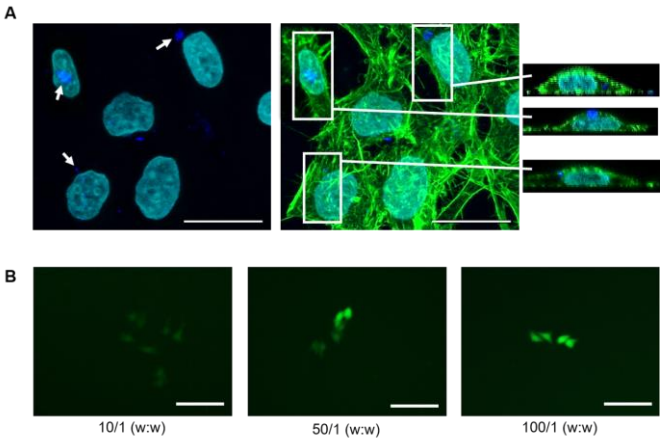

Figure 8. A. Confocal z-stack projections and corresponding lateral views of the internalization with pEGFP-Cy5 after 4 h incubation in SFM. Arrows indicate the positions of dendriplexes. Nuclei were labelled with DAPI (light blue), actin filaments with AlexaFluor 488-Phalloidin (green) and pEGFP with Cy5 (dark blue). Scale bars: 20 µm. B. EGFP expression after 48h transfection with D[G4]-$(NH3^+)_{48}$ (scale = 100 µm).

The efficacy of pEGFP transfection using **D[G4]-$(NH_3^+)_{48}$** as a vector was explored on HeLa cells. The internalization of the dendriplexes was first observed by confocal microscopy after 4 h incubation (Figure 8A). The majority of the complexes (identified with an arrow) were found either at, or passing through the membrane and few were observed on the cytoplasm, indicating a limited internalization. Consequently, transfection levels with **D[G4]-$(NH_3^+)_{48}$** remained low (Figure 8B), with no significant differences on increasing the **D[G4]-$(NH_3^+)_{48}$**/pEGFP ratios. Nevertheless, although a smaller proportion of cells was transfected at a ratio of 100/1, the level of EGFP expression per cell was higher than that obtained at a ratio of 10/1. This result could be related to the rather large size distribution of the complexes.

More interestingly, the efficacy of dendriplexes formed between **D[G4]-$(NH_3^+)_{48}$** and siRNA to reduce specific protein expression was assessed in two different cell lines stably transformed to express an exogenous protein, i.e., a non-tumoral cell line expressing GFP (MDCK-GFP) and a tumoral cell line expressing luciferase (SKOV3-Luc) (Figure 9). siRNA transfection experiments gave positive results on both cell lines, with **D[G4]-$(NH_3^+)_{48}$/siGFP** at a 50/1 ratio (w/w) showing the highest efficacy with a 12% reduction on GFP expression on MDCK-GFP and a 22% reduction on luciferase expression on SKOV3-Luc. In both cases, cell viability after transfection was high, thus proving that the reduction of the protein expression was due to siRNA transfection and not to cell death. The values obtained for dendriplexes at a 50/1 ratio were higher than those found for dendriplexes at a 100/1 ratio, even though not all of the siRNA was complexed with **D[G4]-$(NH_3^+)_{48}$** at the 50/1 ratio. It can be deduced that spherical complexes with a smaller size, close to 60 nm, could be better internalized, which in turn favours a more efficient gene transfection. Compared with commercial transfection agents, these transfection efficacies were similar to those obtained with FuGene (10% GFP expression reduction on MDCK-GFP and 13% reduction of Luciferase on SKOV3-Luc), although not as significant as the reduction achieved with Lipofectamine (79% GFP reduction on MDCK-GFP and 89% reduction of Luciferase on SKOV3-Luc).

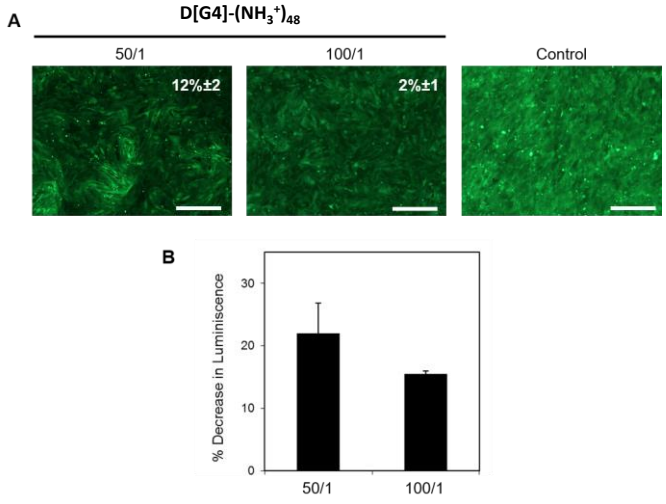

Figure 9. A. Reduction of GFP expression on MDCK-GFP cells after 72h of transfection with **D[G4]-$(NH_3^+)_{48}$** (compared to control cells with 100% expression of GFP). Scale = 500 µm. B. Relative quantification of the reduction of Luciferase expression in SKOV3-Luc after 72h of transfection with **D[G4]-$(NH_3^+)_{48}$**.

Experimental

Materials

Unless otherwise stated, the reagents used for the synthesis of the *bis*-GMPA dendrimers were purchased from Sigma-Aldrich® or Acros Organics™ and were used without further purification. Solvents were purchased from Sigma-Aldrich® or Scharlab, S.L.; dichloromethane was distilled prior to use as a reaction solvent. Camptothecin (CPT) was purchased from Sigma-Aldrich®. Enhanced green fluorescent protein DNA plasmid (pEGFP 4733bp) was obtained from BD Biosciences Clontech®. siRNA duplex targeting green fluorescent protein (siGFP) sequence (GFP Duplex I, 5'-GCA AGC UGA CCC UGA AGU UC-3') and siRNA against luciferase (siLuc) (anti Luciferase I, 5'-GAU UAU GUC CGG UUA UGU AUU-3') were obtained from Thermo Scientific Dharmacon.

Synthesis

Fully details of the synthesis and complete characterization of all the materials are provided in the supplementary information (SI.3 and SI.4). The general procedures carried out for the synthesis of the *bis*-GMPA dendrons and dendrimers and their chemical characterization are described below.

General procedure i): generation growth amidation reaction. The ammonium salt of the corresponding starting dendron (1.00 mol) was dissolved in a mixture of dry dimethylformamide and dry dichloromethane and the *bis*-GMPA monomer (1.20, 1.50 and 1.75 mol per amino group according to the dendron generation), HOBt (1.20, 1.50 and 1.75 mol per amino group according to the dendron generation) and DMAP (1.4 mol per amino group) were added.

The reaction mixture was stirred under argon and cooled down to 0 °C. DCC (1.20, 1.50 and 1.75 mol per amino groups according to the dendron generation) was dissolved in dry dichloromethane and was added drop wise to the reaction mixture. The mixture was stirred at room temperature under argon for 24 h. The white precipitate, N,N'-dicyclohexylurea (DCU), was filtered off and the solvent was evaporated under vacuum to give an orange oil. The remaining DCU and HOBt were precipitated in a mixture of hexane and ethyl acetate and filtered off. The organic phase was washed 3 times with brine, dried over anhydrous $MgSO_4$ and the solvent was evaporated. The remaining HOBt was precipitated into cold ethyl acetate (-16ºC) and filtered off. The solvent was evaporated under reduce pressure. The crude product was purified on silica gel (eluting solvent is detailed with the chemical characterization of each product) to obtain a white product. In the case of the 3rd generation, the crude product was precipitated in a mixture of hexane and ethyl acetate before purification by flash chromatography on silica gel (yields: 74 – 88%).

N_3-[G2]-$(NHBoc)_4$. ^{1}H NMR (400 MHz, $CDCl_3$) δ (ppm): 1.27 (s, 3H, -C$\underline{H}_3$[G1]), 1.29 (s, 6H, –C$\underline{H}_3$[G2]), 1.41 (m, 4H, –CH_2–C$\underline{H}_2$–C$\underline{H}_2$–CH_2–), 1.45 (s, 36H, –$NHCO_2C(C\underline{H}_3)_3$), 1.62 (m, 2H, N_3–CH_2–C$\underline{H}_2$–), 1.67 (m, 2H, –C$\underline{H}_2$–CH_2–OCO–), 3.29 (t, 2H, J = 6.8 Hz, N_3–C$\underline{H}_2$–), 3.91 (d, J = 5.6 Hz, 8H, –C$\underline{H}_2$N–[G2]), 3.98 (d, J = 5.2 Hz, 4H, –C$\underline{H}_2$N–[G1]), 4.15 (t, J = 6.4 Hz, 2H, –$(CH_2)_5$–C$\underline{H}_2$–OCO–), [4.17–4.38] (m, 10 H, –C$\underline{H}_2$O–[G1,2]), 5.29 (bs, –N$\underline{H}$Boc), 7.08 (bs, –N$\underline{H}CO_2$–). ^{13}C NMR (100 MHz, $CDCl_3$) δ (ppm): 17.8, 18.1, 25.4, 26.3, 28.3, 28.7, 41.0, 42.4, 46.1, 46.3, 51.3, 64.9, 65.3, 66.5, 80.1, 155.9, 169.6, 170.3, 172.5, 172.8. MS (MALDI$^+$, DIT) *m/z (%)*: *Found: 1256.8 (100); Calcd. for* $[C_{53}H_{87}N_9O_{24},Na]^+$: *1256.6.* FTIR ($\nu_{max}$/cm^{-1}, ATR): 3379 (N–H st), 2980–2943–2864 (C–H st), 2098 (N_3 st), 1742 (C=O ester st), 1699 (C=O carbamate st), 1676 (C=O amide st), 1520 (N–H δ), 1458 (CH_2, CH_3 δ), 1367 (C–N st), 1246 (CO–O st), 1155 (N–CO–O st). EA (%): *Found:* C, 52.2; H, 7.5; N, 10.1; *Calcd. for* $C_{53}H_{87}N_9O_{24}$: C, 51.6; H, 7.1; N, 10.2. SEC (*ref PMMA*): Mw 1581 g.mol^{-1}; Đ: 1.02.

N_3-[G3]-$(NHBoc)_8$. ^{1}H NMR (400 MHz, $CDCl_3$) δ (ppm): 1.25 (s, 6H, –C$\underline{H}_3$[G2]), 1.26 (s, 3H, –C$\underline{H}_3$[G1]), 1.28 (s, 12H, –C$\underline{H}_3$[G3]), 1.44 (m, 76H, –CH_2–C$\underline{H}_2$–C$\underline{H}_2$–CH_2–, –$NHCO_2C(C\underline{H}_3)_3$), 1.61 (m, 2H, N_3–CH_2–C$\underline{H}_2$–), 1.66 (m, 2H, –C$\underline{H}_2$–CH_2–OCO–), 3.27 (t, 2H, J = 6.8 Hz, N_3–C$\underline{H}_2$–), 3.90 (d, J = 5.2 Hz, 16H, –C$\underline{H}_2$N–[G3]), 3.95 (d, J = 5.2 Hz, 4H, –C$\underline{H}_2$N–[G1]), 4.00 (d, J = 5.2 Hz, 8H, –C$\underline{H}_2$N–[G2]), 4.13 (t, J = 6.4 Hz, 2H, –$(CH_2)_5$–C$\underline{H}_2$–OCO–), [4.20–4.38] (m, 28H, –C$\underline{H}_2$O–[G1,2,3]), 5.42 (bs, –N$\underline{H}$Boc), 7.19 (bs, –N$\underline{H}CO_2$–). ^{13}C NMR (100 MHz, $CDCl_3$) δ (ppm): 17.7, 18.0, 18.3, 25.3, 26.2, 28.3, 28.6, 41.3, 42.3, [46.0–46.1], 51.2, 65.2, 66.4, 80.0, 156.0, 170.6, 172.5, 172.8. MS (MALDI$^+$) *m/z (%)*: *Found: 2578.7 (100); Calcd. for* $[C_{109}H_{175}N_{17}O_{52},Na]^+$: *2578.7.* FTIR ($\nu_{max}$/cm^{-1}, ATR): 3356 (N–H st), 2978–2928–2854 (C–H st), 2106 (N_3 st), 1742 (C=O ester st), 1699 (C=O carbamate st), 1664 (C=O amide st), 1528 (N–H δ), 1458 (CH_2, CH_3 δ), 1367 (C–N st), 1250 (CO–O st), 1157 (N–CO–O st). EA (%): *Found:* C, 51.3; H, 7.3; N, 9.6; *Calcd. for* $C_{109}H_{175}N_{17}O_{52}$: C, 51.2; H, 6.9; N, 9.3. SEC (*ref PMMA*): Mw 2966 g.mol^{-1}; Đ: 1.02.

N_3-[G4]-$(NHBoc)_{16}$. ^{1}H NMR (400 MHz, $CDCl_3$) δ (ppm): [1.24–1.28] (m, 45H, –C$\underline{H}_3$[$G_{1,2,3,4}$]), 1.45 (m, 148H, –CH_2–C$\underline{H}_2$–C$\underline{H}_2$–CH_2–, –$NHCO_2C(C\underline{H}_3)_3$), 1.61 (m, 2H, N_3–CH_2–C$\underline{H}_2$–), 1.66 (m, 2H, –C$\underline{H}_2$–CH_2–OCO–), 3.27 (t, 2H, J = 6.8 Hz, N_3–C$\underline{H}_2$–), 3.88 (m, 32H, –C$\underline{H}_2$N–[G4]), 3.98 (m, 28H, –C$\underline{H}_2$N–[G1,2,3]), 4.11 (t, J = 6.4 Hz, 2H, –$(CH_2)_5$–C$\underline{H}_2$–OCO–), [4.20–4.45] (m, 60H, –C$\underline{H}_2$O–[G1,2,3,4]), 5.55 (bs, –N$\underline{H}$Boc), 7.19 (bs, –N$\underline{H}CO_2$–). ^{13}C NMR (100 MHz, $CDCl_3$) δ (ppm): [17.7–18.0], 25.3, 26.3, 28.3, 28.6, 41.3, 42.3, [46.0–46.1], 51.3, 65.3, [66.3–66.5], 80.0, 156.1, 169.6, [170.2–170.3], 172.6, [172.9–173.2]. MS (MALDI$^+$, DCTB) *m/z (%)*: *Found: 5220.2 (100); Calcd. for* $[C_{221}H_{351}N_{33}O_{108},Na]^+$: *5218.3.* FTIR ($\nu_{max}$/cm^{-1}, ATR): 3362 (N–H st), 2978–2930–2852 (C–H st), 2098 (N_3 st), 1749 (C=O ester st), 1695 (C=O carbamate st), 1668 (C=O amide st), 1520 (N–H δ), 1456 (CH_2, CH_3 δ), 1367 (C–N st), 1284 (CO–O st), 1155 (N–CO–O st). EA (%): *Found:* C, 52.2; H, 7.1; N, 8.8; *Calcd. for* $C_{221}H_{351}N_{33}O_{108}$: C, 51.1; H, 6.8; N, 8.9. SEC (*ref PMMA*): Mw 4463 g.mol^{-1}; Đ: 1.04.

General procedure ii): deprotection of the terminal amino groups. *t*-Boc protected dendron (1 mol) was dissolved in ethyl acetate. A saturated solution of HCl in ethyl acetate was carefully added to it. The reaction mixture was stirred at room temperature during 1 hour and a white precipitate formed. The reaction mixture was diluted in ethyl acetate and was stirred for an additional 30 min. The mixture was stirred under vacuum to remove the hydrochloric acid vapours. The white residue was recovered by centrifugation and was washed twice with pure ethyl acetate (yields: 81 – 93%).

N_3-[G2]-$(NH_3^+)_4$. ^{1}H NMR (400 MHz, CD_3OD) δ (ppm): 1.27 (s, 3H, –C$\underline{H}_3$[G1]), 1.37 (s, 6H, –C$\underline{H}_3$[G2]), 1.43 (m, 4H, –CH_2–C$\underline{H}_2$–C$\underline{H}_2$–CH_2–), 1.62 (m, 2H, N_3–CH_2–C$\underline{H}_2$–), 1.69 (m, 2H, –C$\underline{H}_2$–CH_2–OCO), 3.93 (m, 8H, –C$\underline{H}_2$N–[G2]), 3.96 (m, 4H, –C$\underline{H}_2$N–[G1]), 4.16 (t, J = 6.4 Hz, 2H, –$(CH_2)_5$–C$\underline{H}_2$–OCO–), 4.32 (ABq, J = 11.6 Hz, $\Delta\nu_{AB}$ = 9.4 Hz, 4H, –C$\underline{H}_2$O–[G1]), 4.45 (ABq, J = 11.2 Hz, 8H, –C$\underline{H}_2$O–[G_2]); note: N_3–C$\underline{H}_2$– signal (~3.2 ppm) is overlapped with the signal of C$\underline{H}_3$OD, nevertheless the correlation between N_3–C$\underline{H}_2$–CH_2– and N_3–CH_2–C$\underline{H}_2$– is observed in ^{1}H-^{1}H COSY as well as the correlation between N_3–C$\underline{H}_2$– and N_3–$\underline{C}H_2$– is observed in ^{1}H-^{13}C HSQC. ^{13}C NMR (100 MHz, CD_3OD) δ (ppm): 17.8, 18.1, 26.5, 27.3, 29.4, 29.7, 41.1, 42.1, 47.3, 47.6, 52.3, 66.6, 67.2, 68.5, 168.2, 170.9, 174.0, 174.9. MS (MALDI$^+$, DIT) *m/z (%)*: *834.7 (100); Calcd. for* $[C_{33}H_{55}N_9O_{16},Na]^+$: *834.4*. FTIR ($\nu_{max}$/cm^{-1}, ATR): 3600–2600 (bs N–H$^+$ st), 3222 (N–H st), 2941–2861 (C–H st), 2098 (N_3 st), 1747 (C=O st ester), 1662 (C=O st amide and N–H$^+$ δ), 1541 (N–H δ), 1478 (CH_2, CH_3 δ), 1407 (C–N st), 1246 (ν_{as} CO–O), 1138 (O–C–C st). EA (%): *Found:* C, 39.9; H, 6.5; N, 12.9. *Calc. for* $C_{33}H_{59}Cl_4N_9O_{16}$: C, 40.5; H, 6.1; N, 12.9.

N_3-[G3]-$(NH_3^+)_8$. ^{1}H NMR (400 MHz, CD_3OD) δ (ppm): 1.28 (s, 3H, –C$\underline{H}_3$[G1]), 1.33 (s, 6H, –C$\underline{H}_3$[G2]), 1.38 (s, 12H, –C$\underline{H}_3$[G3]), 1.43 (m, 4H, –CH_2–C$\underline{H}_2$–C$\underline{H}_2$–CH_2–), 1.62 (m, 2H, N_3–CH_2–C$\underline{H}_2$–), 1.69 (m, 2H, –C$\underline{H}_2$–CH_2–OCO), 3.93 (s, 16H, –C$\underline{H}_2$N–[G3]), 3.97 (s, 4H, –C$\underline{H}_2$N–[G1]), 4.01 (s, 8H, –C$\underline{H}_2$N–[G2]), 4.16 (t, J = 6.4 Hz, 2H, –$(CH_2)_5$–C$\underline{H}_2$–OCO–), 4.32 (m, 14H, –C$\underline{H}_2$O–[G1,2]), 4.45 (ABq, 16H, –C$\underline{H}_2$O–[G3]). ^{13}C NMR (100 MHz, CD_3OD) δ (ppm): 17.8, 18.1, 26.6, 27.4, 29.4, 29.8, 41.2, 42.2, 47.4, 47.7, 52.4, 66.5, 67.2, 67.8, 68.5, 168.3, 170.8, 171.1, 174.1, 175.0, 175.2. FTIR (ν_{max}/cm^{-1}, ATR): 3600–2600 (bs N–H$^+$ st), 3342 (N–H st), 2984–2928 (C–H st), 2091 (N_3 st), 1755 (C=O st ester), 1659 (C=O st amide and N–H$^+$ δ), 1541 (N–H δ), 1475 (CH_2, CH_3 δ),

1406 (C–N st), 1236 (ν_{as} CO–O), 1171 (O–C–C st). EA (%): *Found:* C, 39.7; H, 6.5; N, 11.5. *Calc. for* $C_{69}H_{119}Cl_8N_{17}O_{36}$: C, 40.5; H, 5.9; N, 11.6.

N_3-[G4]-(NH_3^+)$_{16}$. ^{1}H NMR (400 MHz, CD_3OD) δ (ppm): 1.23 (s, 3H, –C*H*$_3$[G1]), 1.28 (s, 6H, –C*H*$_3$[G2]), 1.33 (s, 12H, –C*H*$_3$[G3]), 1.38 (s, 24H, –C*H*$_3$[G4]), 1.43 (m, 4H, –CH_2–C*H*$_2$–C*H*$_2$–CH_2–), 1.62 (m, 2H, N_3–CH_2–C*H*$_2$–), 1.69 (m, 2H, –C*H*$_2$–CH_2–OCO), 3.95 (m, 32H, –C*H*$_2$N–[G4]), 4.01 (m, 4H, –C*H*$_2$N–[G1,2,3]), 4.16 (t, J = 6.4 Hz, 2H, –$(CH_2)_5$–C*H*$_2$–OCO–), 4.33 (m, 28H, –C*H*$_2$O–[G1,2,3]), 4.46 (m, 32H, –C*H*$_2$O–[G4]), 8.35 (bs, –N*H*CO_2–). ^{13}C NMR (100 MHz, CD_3OD) δ (ppm): [17.9–18.2], 26.6, 27.4, 29.4, 29.8, 41.2, 42.2, [47.3–47.7], 52.4, 66.4, [67.2–67.9], 68.5, 168.3, [170.8–171.3], 174.2, [174.9–175.3]. FTIR (ν_{max}/cm^{-1}, ATR): 3600–2600 (bs N–H$^+$ st), 3318 (N–H st), 2986–2883 (C–H st), 2102 (N_3 st), 1744 (C=O st ester), 1655 (C=O st amide and N–H$^+$ δ), 1539 (N–H δ), 1479 (CH_2, CH_3 δ), 1410 (C–N st), 1230 (ν_{as} CO–O), 1176 (O–C–C st). EA (%): *Found:* C, 39.4; H, 6.5; N, 10.7. *Calc. for* $C_{141}H_{239}Cl_{16}N_{33}O_{76}$: C, 40.5; H, 5.8; N, 11.1.

General procedure iii): dendrimer synthesis by means of CuAAC. Tripropargylamine (1.00 mol) and *t*-Boc protected *bis*-GMPA dendron (1.10 mol per alkyne group) were dissolved in dimethylformamide (7 mL) in a Schlenk flask. Three vacuum-argon cycles were carried out to flush the flask from air. The reaction mixture was stirred under argon at 45 °C. $CuSO_4$, $5{\cdot}H_2O$ (0.5 mol per alkyne group), L-ascorbate (1.0 mol per alkyne group) and TBTA (0.1 mol per alkyne group) were dissolved into dimethylformamide (3 mL) in a second Schlenk flask. 3 cycles vacuum-Argon were made in order to flush the flask from air. The copper solution was stirred at 45 °C during 15 min and was then added through a cannula to the azide-alkyne reaction mixture. The reaction mixture was stirred at 45 °C for 2 days. Brine (100 mL) was added and the product was extracted twice with ethyl acetate (2 x 70 mL). The organic phase was washed three times with brine (3 x 100 mL), once with aqueous KCN solution (15 mg in 100 mL of water) and twice with brine (2 x 100 mL), dried over anhydrous $MgSO_4$ and the solvent was evaporated under reduced pressure. The crude product was precipitated in a mixture of hexane and ethyl acetate (4:6 for D[G3]-$(NHBoc)_{24}$ and 5:5 for D[G4]-$(NHBoc)_{48}$, 100 mL); the crude product was first dissolved in ethyl acetate and hexane was slowly added to the solution. The product was recovered by centrifugation and the solid was washed once with the same mixture of hexane and ethyl acetate. Finally, the product was dialyzed against methanol (cellulose acetate, MW 1000 Da) to give a white or pale yellow powder. The terminal *t*-Boc protective groups were removed under acidic conditions, as explained in general procedure ii) (yields: 75 – 88%).

D[G3]-(NH_3^+)$_{24}$. ^{1}H NMR (500 MHz, CD_3OD) δ (ppm): 1.28 (s, 9H, –C*H*$_3$[G1]), 1.33 (s, 18H, –C*H*$_3$[G2]), 1.38 (s, 36H, –C*H*$_3$[G3]), 1.43 (m, 12H, –CH_2–C*H*$_2$–C*H*$_2$–CH_2–), 1.68 (m, 6H, –C*H*$_2$–CH_2–OCO), 1.99 (m, 6H, –$C_2H_1N_3$–CH_2–C*H*$_2$–), 3.95 (s, 48H, –C*H*$_2$N-[G3]), 3.97 (s, 12H, –C*H*$_2$N-[G1]), 4.01 (s, 24H, –C*H*$_2$N–[G2]), 4.15 (m, 6H, –$(CH_2)_5$–C*H*$_2$–OCO), 4.33 (m, 36H, –C*H*$_2$O–[G1,2]), 4.46 (m, 48H, –C*H*$_2$O–[G3]), 4.52 (m, 12H, N–C*H*$_2$–$C_2H_1N_3$–C*H*$_2$–), 8.30 (bs, –N*H*CO_2–), 8.42 (s, 3H, –$C_2H_1N_3$–). ^{13}C NMR (125 MHz, CD_3OD) δ (ppm): [17.9–18.2], 26.4, 27.1, 29.4, 31.2, 41.2, 42.2, [47.4–47.5], 47.7, 51.6, 66.4, [67.2–68.6], 128.7, 137.9, 168.3, [170.8–175.2]. FTIR (ν_{max}/cm^{-1}, ATR): 3600–2600 (bs N–H$^+$ st), 2947–2633 (C–H st), 1749 (C=O st ester), 1655 (C=O st amide and N–H$^+$ δ), 1545 (N–H δ), 1473 (CH_2, CH_3 δ), 1379 (C–N st), 1221 (CO–O st).

D[G4]-(NH_3^+)$_{48}$. ^{1}H NMR (500 MHz, CD_3OD) δ (ppm): 1.23 (s, 9H, –C*H*$_3$[G1]), 1.28 (s, 18H, –C*H*$_3$[G2]), 1.33 (s, 36H, –C*H*$_3$[G3]), 1.38 (s, 72H, –C*H*$_3$[G4]), 1.45 (m, 12H, –CH_2–C*H*$_2$–C*H*$_2$–CH_2–), 1.68 (m, 6H, –C*H*$_2$–CH_2–OCO–), 1.99 (m, 6H, –$C_2H_1N_3$–CH_2–C*H*$_2$–), 3.96 (s, 96H, –C*H*$_2$N–[G4]), 4.01 (m, 84H, –C*H*$_2$N–[G1,2,3]), 4.15 (m, 6H, –$(CH_2)_5$–C*H*$_2$–OCO), 4.33 (m, 84H, –C*H*$_2$O–[G1,2,3]), 4.46 (m, 96H, –C*H*$_2$O–[G4]), 4.56 (m, 12H, N–C*H*$_2$–$C_2H_1N_3$–C*H*$_2$–), 8.30 (bs, –N*H*CO_2–), 8.44 (s, 3H, –$C_2H_1N_3$–). ^{13}C NMR (125 MHz, CD_3OD) δ (ppm): [17.9–18.2], 26.4, 27.1, 29.4, 31.2, 41.2, 42.3, [47.4–47.5], 47.7, 51.6, 65.7, [66.4–68.6], 128.9, 137.7, 168.3, [170.9–177.0]. FTIR (ν_{max}/cm^{-1}, ATR): 3600–2600 (bs N–H$^+$ st), 3391 (N–H st), 2935–2615 (C–H st), 1749 (C=O st ester), 1655 (C=O st amide and N–H$^+$ δ), 1545 (N–H δ), 1477 (CH_2, CH_3 δ), 1385 (C–N st), 1211 (CO–O st).

Chemical Characterization.

^{1}H NMR and ^{13}C NMR experiments were performed on Bruker AMX-300 (^{1}H: 300 MHZ, ^{13}C: 75 MHz), Bruker AV-400 (^{1}H: 400 MHz, ^{13}C: 100 MHz) or Bruker AV-500 (^{1}H: 500 MHz, ^{13}C: 125 MHz) spectrometers employing deuterated chloroform ($CDCl_3$), deuterated methanol (CD_3OD) or deuterated water (D_2O) as solvents. The chemical shifts are given in ppm relative to TMS and the coupling constants in Hz; the solvent residual peak was used as internal standard. Mass spectrometry (MS) was performed with a Bruker Microflex employing the MALDI-TOF technique with nitrogen laser (337 nm) and dithranol (DIT), 2,5-dihydroxybenzoic acid (DHB) or *trans*-2-[3-(4-*tert*-butylphenyl)-2-methyl-2-propenylidene]malononitrile (DCTB) as matrix, and sodium trifluoroacetic acid as cationic agent or with an ESI Bruker Esquire 3000 plus spectrometer employing the electrospray technique. Infrared spectra were obtained on a Bruker Vertex 70 spectrophotometer in ATR mode and recorded between 4000 and 800 cm^{-1} or using an FTIR ATI-Mattson Genesis series II system while the sample was suspended in nujol in NaCl cells and recorded between 4000 cm^{-1} and 600 cm^{-1}. Size exclusion chromatography was performed on a Waters e2695 Alliance system employing two in series Styragel columns HR4 and HR1 (500 and 10^4 Å of pore size) and a Waters 2424 evaporation light scattering detector with a sample concentration of 1.00 mg/mL. The solvent was THF (HPLC grade) with a flow rate of 1.00 mL/min at 35 °C; PMMA was used as the standard for calibration. Elemental Analysis (EA) was performed with a Perkin-Elmer 2400 series II microanalyser.

Microscopy

Transmission electron microscopy (TEM) and cryogenic transmission electron microscopy (cryoTEM) images were obtained with a FEI TECNAI T20 with a beam power of 200 kV. For TEM, a droplet of the sample was deposited on a holey carbon film 300 mesh coppered grid (Agar Scientific Ltd) and was allowed to penetrate for 30 seconds; the excess was

View Article Online
DOI: 10.1039/C8TB00670C

removed using a filter paper. A phosphotungstic acid aqueous solution (3%) was used as negative stain; a droplet of the stain solution was deposited on the sample grid, allowed to penetrate during 10 seconds and the excess was removed using a filter paper. The grid was dried for at least 24 hours at atmospheric pressure. The average size of the different aggregates measured by TEM was obtained by comparing at least 100 aggregates in at least 5 photos.

For CryoTEM, a droplet of the sample was deposited on Lacey carbon film 300 mesh coppered grids (Agar Scientific Ltd) previously ionized by glow discharge. Sample vitrification was automatically processed using a vitrobot (FEI) and performed in liquid ethane. A specific holder, Gatan for cold samples, was used to stock the grids in liquid nitrogen between sample vitrification and microscope observation.

Atomic force microscopy (AFM) images were obtained in liquid medium on a Veeco MultiMode 8 with a cantilever with a force constant of 0.7 Nm^{-1} (Bruker) at 1 Hz, in tapping mode (150 kHz). Samples (20 μL) were deposited onto a previously exfoliated mica substrate. Before adding the samples, $MgCl_2$ (10 mM) was added to the mica substrate to favour adsorption for 1 minute and then the substrates were rinsed three times with milliQ water.

Dendron degradation

Bis-GMPA dendrons (10 mg) were dissolved in a mixture of 4.5 mL of the corresponding aqueous buffer solution (phosphate buffered saline, pH =7.4, or citric acid–sodium citrate buffer, pH = 5.0) and 0.5 mL of deuterated water. The different samples were heated at 37 °C and ^{1}H NMR spectra were recorded at different times in an AV 500 spectrometer using the Excitation Sculpting pulse sequence for water suppression.

Dendrimer/drug association.

The solvent diffusion technique was carried out to associate camptothecin (CPT) and **D[G3]-(NH_3^+)$_{24}$**. First, 200 μg/mL of CPT in DMSO were added to the aqueous dendrimer solution (1 mg/mL in distilled water) according to a feeding ratio of 100 μg of CPT per mg of dendrimer. The mixture was stirred at 4 °C for 16 hours to allow the formation of dendrimer/drug aggregates. DMSO was removed by dialysis against distilled water at 4 °C (cellulose acetate, 1000 Da cut-off). The non-associated drug precipitated during the dialysis and was removed by filtration (cellulose acetate, 0.2 μm) in order to obtain the dendrimer/drug conjugate. The concentration of associated CPT was directly measured by fluorescence (λ_{max} = 436 nm and λ_{ext} = 368 nm, Perkin-Elmer-LS 55 system) in a mixture of DMSO/H_2O (9/1). This process was carried out in duplicate.

Isothermal titration calorimetry (ITC) assay. The interaction of CPT with **D[G3]-(NH_3^+)$_{24}$** was studied by ITC using a high sensitivity isothermal titration VP-ITC microcalorimeter (MicroCal, USA). Experiments were performed at 25 °C in aqueous media. A 10 μM solution of dendrimer was placed in the calorimetric cell and titrated with sequential injections of a 100 μM solution of CPT. Control experiments were performed under the same experimental conditions. The heat evolved after each injection was obtained from the integral of the calorimetric signal. The heat due to the binding reaction was obtained as the difference between the reaction heat and the corresponding heat of dilution, the latter estimated as a constant heat throughout the experiment, and included as an adjustable parameter in the analysis. The association constant (Ka) and the enthalpy change (ΔH) were obtained through non-linear regression of experimental data to a model considering one class of ligand binding sites. Data were analysed using software developed in our laboratory and implemented in Origin 7 (OriginLab, USA).

Cells and replicon system.

The highly permissive cell clone Huh /-Lunet, as well as HuH 7 cells containing subgenomic (HCV) replicons I389luc-ubi-neo/NS3-3'/5.1 (Huh 5-2), I377NS3-3'/wt (Huh 9-13), or I389/hygro-ubi-NS3-3'/5.1 (a kind gift from Dr. V. Lohmann and Dr. R. Bartenschaler) has been described.[29,30] Briefly, this system allowed the efficient propagation of genetically modified HCV RNAs (replicons) in a human hepatoma cell line (Huh). The amount of RNA that has been transcribed and translated is determined through the quantification of a reporter contained the replicon system (luciferase). The amount of luminescence detected (after adding the substrate specific for this enzyme) is proportional to the virus replication rate (references). Cells were grown in a DMEM supplemented with 10% heat-inactivated fetal bovine serum 1 x non-essential amino acids, 100 IU/mL penicillin, 100 μg/mL streptomycin and 250 μg/mL geneticin (G418).

Antiviral and cytostatic assays with Huh 5-2 cells

Antiviral and cytostatic assays were performed according to the protocol already described by us in reference 27. Full details are included in the SI (SI.1.). The 50% effective concentration (EC50) was defined as the concentration of compound that reduced the luciferase signal by 50 % and the 50% cytotoxic concentration (CC50) was determined employing the dose‑response equation (i.e., Hill equation).

Dendriplexes formation, size and ζ potential of the dendriplexes.

Dendriplexes were freshly prepared before used. Briefly, pDNA or siRNA was added to a series of dendrimer solutions and were mixed by vigorous pipetting and incubated for 20 min at room temperature.

Gel Retardation Assay. 15 μL of dendriplexes at different ratios, from 1/1 to 200/1 (w/w), containing 250 ng of pDNA or ratios w/w 1-80 and 0.3 μg siRNA, were mixed with appropriate amounts of 6X loading buffer (Takara, UK) and then electrophoresed on a 0.8% (w/v) agarose gel in 1X TAE (40 mM TRIS/HCl, 1% acetic acid, 1 mM EDTA, pH 7.4) containing SyberSafe for 30 min at 95V. The location of pDNA and siRNA in the gel was analysed on a G:Box UV transilluminator (Syngene, UK).

Dynamic light scattering (DLS). Measurements were performed with Brookhaven instruments Corporation 90 plus particle size analyser. Samples for DLS measurements were freshly prepared in distilled water at a concentration of 1.00

mg/mL at two dendrimers:pDNA (w/w) ratios (10/1 and 100/1) and at one dendrimer:siRNA (w/w) ratio 100/1. A series of 3 measurements were performed for each sample. Results are given in intensity.

ζ potential titration. Measurements were performed with a Malvern Zetasizer Nano ZS in a NaCl-HEPES buffer containing 6 mM of HEPES buffer pH 7.4 and 144 mM of NaCl. The dendriplexes were freshly prepared at a concentration of 10 $\mu g \cdot mL^{-1}$ of pDNA or siRNA and various dendrimer concentrations. Three measurements with a minimum of 10 scans were carried out for each sample.

Cell lines and cell culture

mMSCS were grown in DMEM/F12 (Biowest) supplemented with 10% FBS (Gibco), 1%Penicillin/Streptomycin/Amphotericin (Biowest) and 2 mM L-glutamine (Biowest) and maintained under hypoxic conditions (3% O_2). HeLa, MDCK-GFP (Madin-Darby Canine Kidney stably expressing GFP) and SKOV3-Luc derived from human ovarian carcinoma and stably expressing Luciferase (kindly obtained from Cancer Research-UK Cell services) were maintained in DMEM High Glucose (w/Glutamine, Biowest) supplemented with 10% FBS and 1% Pencillin/ Streptomycin/Amphotericin at 37 °C and 5% CO_2 in a humidified atmosphere. Cells were treated and analysed as indicated for each experiment.

In vitro transfection and biocompatibility.

For cytotoxicity evaluation, cells were seeded at a density of 5 × 10^3 cells per well in 96 multiwell culture plates. After 24 h incubation, the culture medium was removed and 100 μL of DMEM with increasing concentrations of the corresponding dendrimer were added (0.1–1 mg/mL). After 24–72 h the solutions were replaced by 100 μL of fresh DMEM and 10 μL of Alamar Blue® dye solution (Thermo Fisher Scientific). After incubation for 3 h at 37 ºC, fluorescence was read at 530/590 (excitation/emission) on a Synergy HT (BioTek, USA) plate reader. Untreated cells incubated with medium without dendrimer were used as control and cytotoxicity is expressed as the relative viability of the cells compared to control cells (considered as 100% viability). Four replicates per concentration were assayed for each of the three independent experiments performed. Also, DNA cell cycle analysis was measured on propidium iodide (PI)-stained nuclei of 10^6 cells using a FACS Array system (Becton Dickinson). For all the experiments, the control and sample cells were harvested by trypsinisation, washed twice with PBS, fixed in ice-cold 70% EtOH and maintained at 4 °C for at least 1 h prior to analysis.

For pEGFP transfection, cellular uptake and internalization, experiments were carried out on mMSCs and HeLa cells as previously described by us.[28] Full details are included in the SI (SI.2.)

Dendriplexes formed with 100-400 nM siGFP or siLuc in serum free media (SFM) were incubated for 4 h with MDCK-GFP or SKOV3-Luc cells seeded at a density of $1 \cdot 10^4$ cells per well in 96-well plates. For the positive controls, cells were incubated with Fugene at ratio of 3/1 (w/w). EGFP expression was first evaluated by fluorescence microscopy (Olympus IX81 Olympus, Spain) at 72 h. For quantification of EGFP by flow cytometry, cells were seeded at a density of $5 \cdot 10^5$ cells per well in 6-well plates and incubated with 750 μL of dendriplexes with 200 nM siGFP for 4h. For quantification of Luciferase with Bright-Glo™ Assay Reagent (Promega), after 72 h of transfection with siLuc, the medium was changed for 100 μL fresh DMEM, 100 μL of Bright-Glo™ Assay Reagent (lysis buffer and luciferin) were added and cells were lysed by pipetting. After 5 min all the contents were transferred to an opaque 96 well plate (Nunc) in the dark. Luminescence was read on a Synergy HT system (Biotek).

Statistical analysis

Results are reported as mean ± SD and experiments were performed at least in triplicate. Normally distributed data were analysed by two-sample t-test and one-way ANOVA using Minitab 17 software (State College, PA). $p < 0.01$ (**) and $p < 0.05$ (*) were considered to be statistically significant.

Conclusions

A two-step iterative synthetic procedure that consists of amide coupling and *t*-Boc cleavage reactions involving a novel 2,2´-*bis*(glycyloxy)propionic acid (*bis*-GMPA) monomer allowed the synthesis of cationic poly(ester amide) dendrons. Following a convergent strategy based on CuAAC click-chemistry, these dendrons provide cationic tripodal dendrimers of 3rd and 4th generation, with 24 and 48 terminal amino groups respectively, in good yields. These dendrimers were found to be fully biocompatible and degradable in water by hydrolysis. They have demonstrated their potential for use as drug delivery systems as they could enhance the cell viability and the anti-HCV activity of camptothecin. On the other hand, these materials can spontaneously form dendriplexes with both pDNA and siRNA. Effective *in vitro* siRNA transfection was observed into tumoral and non-tumoral cells. These positive results reveal that ammonium-terminated poly(ester amide) dendrimers are an interesting option for the design of carriers for a broad range of therapeutic applications (drug delivery and gene therapy).

Conflicts of interest

There are no conflicts of interest to declare.

Acknowledgements

This work was financially supported by the MINECO-FEDER funds (under the projects CTQ2015-70174-P and MAT2015-66208-C3-1-P), Miguel Servet Program from the Instituto de la Salud Carlos III (CPII13/00017 to O.A.), Instituto de Salud Carlos III and European Union (ERDF/ESF, "Investing in your future") (PI15/00663) and the Gobierno de Aragón-FSE (E04 and B01 research groups). Centro de Investigacion Biomédica en Red en Enfermedades Hepaticas y Digestivas (CIBERehd);

and Asociación Española de Gastroenterologia (AEG). A.L. and R.C-G thank the MECD for their FPU grants (FPU12/05210 and FPU13/3870). R.G.-P. and R.C-G thank the DGA for their EPIF grants. The authors are grateful to Dr. A. Gonzalez-Orive and Dr. H.M. Osorio for their help with AFM studies, and M. Savirón for her help with MS spectrometry studies. The authors would like to acknowledge the use of Servicios Científico-Técnicos of CEQMA (Universidad de Zaragoza-CSIC), Servicio General de Apoyo a la Investigación-SAI (Universidad de Zaragoza), microscopy, cell culture and cytometry departments at CIBA (IACS-Universidad de Zaragoza) and the LMA (INA-Universidad de Zaragoza).

References

1 V.P. Torchilin, *Nat. Rev. Drug. Discov.* 2014, **13** (11), 813—827.
2 K. Ulbrich, K. Holá, V. Šubr, A. Bakandritsos, J. Tuček, R. Zbořil, *Chem. Rev.* 2016, **116** (9), 5338—5431.
3 M. Hamidi, A. Azadi, P. Rafiei, H. Ashrafi, *Crit. Rev. Ther. Drug Carrier Syst.* 2013, **30** (5), 435—467.
4 M.A. Kay *Nat. Rev. Gen.* 2011, **12** (5), 316—328.
5 H. Yin, R.L. Kanasty, A.A. Eltoukhy, A.J. Vegas, J.R. Dorkin, D.G. Anderson, *Nat. Rev. Genet.* 2014, **15** (8), 541—555.
6 a) J. Nicolas, S. Mura, D. Brambilla, N. Mackiewicz, P. Couvreur, *Chem. Soc. Rev.* 2013, **42** (3), 1147—1235. b) I. Ullah, K. Muhammad, M. Akpanyung, A. Nejjari, A. L. Neve, J. Guo, Y. Feng and C. Shi, *J. Mater. Chem. B*, 2017, **5**, 3253—3276.
7 F. Vögtle, G. Richardt, N. Werner, Dendrimer Chemistry: Concepts, Syntheses, Properties, Applications. 2009 WILEY-VCH Verlag GmbH & Co. Weinheim.
8 H.J. Hsu, J. Bugno, S.R. Lee, S. Hong, *WIREs Nanomed. Nanobiotechnol.* 2017, **9** (1), e1409.
9 L. Palmerston Mendes, J. Pan and V. Torchilin, *Molecules*, 2017, **22**, 1401.
10 J. Yang, Q. Zhang, H. Chang, Y. Cheng, *Chem. Rev.* 2015, **115** (11), 5274–5300.
11 R.M. Kannan, E. Nance, S. Kannan, D.A. Tomalia, *J. Intern. Med.* 2014, **276** (6), 576–617.
12 R. Esfand, D.A. Tomalia, *Drug Discov. Today* 2001, **6** (8), 427–436.
13 C. Luo, D. Lü, J. Pan, L. Mian, *ACS Appl. Mater. Interfaces* 2016, **8** (13), 8367–8375.
14 B.H. Zinselmeyer, S.P. Mackay, A.G. Schatzlein, I.F. Uchegb, *Pharm. Res.* 2002, **19** (7), 960–967.
15 M. Labieniec-Watala, C. Watala, *J. Pharm. Sci.* 2015, **104** (1), 2–14.
16 D. Luong, P. Kesharwani, R. Deshmukh, M.C.I.M. Amin, U. Gupta, K. Greish, A.K. Iyer, *Acta Biomaterialia*, 2016, **43**, 14–29.
17 S. Thakur, R.K. Tekade, P. Kesharwani, N.K. Jain, *J. Nanopart. Res.* 2013, **15** (5), 1625.
18 A. Carlmark, E. Malmström, M. Malkoch, *Chem. Soc. Rev.* 2013, **42** (13), 5858–5879.
19 M. Calderón, M.A. Quadir, S.K. Sharma, R. Haag, *Adv. Mater.* 2010, **22** (2), 190–218.
20 J. Movellan, R. González-Pastor, P. Martín-Duque, T. Sierra, J.M. de la Fuente, J.L. Serrano, *Macromolecular Biosci.* 2015, **15** (5), 657–667.
21 S. Jain, A. Kaur, R. Puri, P. Utreja, A. Jain, M. Bhide, R. Ratnam, V. Singh, A.S. Patil, N. Jayaraman, G. Kaushik, S. Yadav, K.L. Khanduja, *Eur. J. Med. Chem.* 2010, **45** (11), 4997–5005.
22 A. Lakshminarayanan, V.K. Ravi, R. Tatineni, Y.B. Rajesh, V. Maingi, K.S. Vasu, N. Madhusudhan, P.K. Maiti, A.K. Sood, S. Das, N. Jayaraman, *Bioconjug. Chem.* 2013, **24** (9), 1612–1623.
23 A. Sousa-Herves, R. Novoa-Carballal, R. Riguera, E. Fernandez-Megia, *AAPS J.* 2014, **16** (5), 948–961.
24 A.C. Fonseca, M.A. Gil, P.M. Simões, *Prog. Polym. Sci.* 2014, **39** (7), 1291–1311.
25 D. Pahovnik, A. Čusak, S. Reven, E. Žagar, *J. Polym. Sci. Part A: Polym. Chem.* 2014, **52** (22), 3292–3301.
26 J. Movellan, P. Urbán, E. Moles, J.M. de la Fuente, T. Sierra, J.L. Serrano, X. Fernàndez-Busquets, *Biomaterials* 2014**, 35** (27), 7940–7950.
27 A. Lancelot, R. Clavería-Gimeno, A. Velázquez-Campoy, O. Abián, J.L. Serrano, T. Sierra, *Eur. J. Pol.* 2017, **90**, 136–149.
28 A. Lancelot, R. González-Pastor, A. Concellón, T. Sierra, P. Martín-Duque, J.L. Serrano, *Bioconjugate Chem.* 2017, **28** (4), 1135–1150.
29 K.J. Blight, J.A. Mc Keating, C.M. Rice, *J. Virol.* 2002**, 76** (24), 13001–13004.
30 V. Lohmann, F. Kormer, J. Koch, U. Herian, L. Theilmann, R. Bartenschlager, *Science* 1999**, 285** (5424) 110-113.
31 E. Fedeli, A. Lancelot, J.L. Serrano, P. Calvo, T. Sierra, *New J. Chem.* 2015, **39** (3), 1960-1967.
32 a) L. Wang, D.J. Kiemle, C.J. Boyle, E.L. Connors, I. Gitsov, *Macromolecules* 2014, **47** (7), 2199-2213; b) F. Barmare, M.-C. Abadjian, E.C. Wiener, D.B. Grotjahn, *J. Org. Chem.* 2016, **81** (15), 6779-6782.
33 a) J.W. Lee, B.K. Kim, *Korean Chem. Soc.* 2005, **6** (4), 658–660 b) M.D. Hossain, D. Valade, Z. Jia, M.J. Montero, *Polym. Chem.* 2012, **3** (10), 2986-2995.
34 Dietary Reference Intakes Tables and Applications: Table DRI Values Summary-A. *The National Academy of Sciences, Engineering Medicine*.
35 O. Abian, S. Vega, J. Sancho, A. Velázquez-Campoy, *PLoS ONE* 2013, **8**, e69773.
36 I. Jiménez-Pardo, R. González-Pastor, A. Lancelot, R. Clavería-Gimeno, A. Velázquez-Campoy, O. Abián, M.B. Ros, T. Sierra, *Macromol. Biosci.* 2015, **15** (10), 1381–1391.
37 A. Concellón, R. Clavería-Gimeno, A. Velázquez-Campoy, O. Abian, M. Piñol, L. Oriol, *RSC Adv.* 2016, **6** (29), 24066–24075.
38 D. Grimm, M.A. Kay, *ASH Education Program Book*. 2007**, 1**, 473–481.
39 M. Ramamoorth, A. Narvekar, *J. Clin. Diagn. Res*. 2015, **9** (1), GE01–GE06.
40 L. De Laporte, J.C. Rea, L.D. Shea, *Biomaterials* 2006, **27** (7), 947–954.
41 M. Xu, J. Qian, A. Suo, N. Cui, Y. Yao, W. Xu, T. Liu, H. Wang, *J. Mater. Chem. B*. 2015, **3** (10), 2215–2228.
42 L. Albertazzi, F.M. Mickler, G.M. Pavan, F. Salomone, G. Bardi, M. Panniello, E. Amir, T. Kang, K.L. Killops, C. Bräuchle, R.J. Amir, C.J. Hawker, *Biomacromolecules* 2012, **13** (12), 4089–4097.

View Article Online
DOI: 10.1039/C8TB00639C

Cationic poly(ester amide) dendrimers: alluring materials for biomedical applications

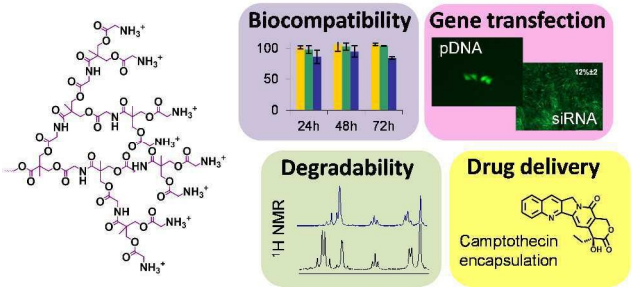

Cationic poly(ester amide) dendrons that constitute an interesting option for the design of biocompatible and biodegradable dendritic nanocarriers for therapeutic applications.